Microwave Spectrum, Structure, and Internal Dynamics of the Nitric Acid Dihydrate Complex

Matthew B. Craddock,† Carolyn S. Brauer,‡ and Kenneth R. Leopold*

Department of Chemistry, University of Minnesota, 207 Pleasant Street SE, Minneapolis, Minnesota 55455

Received: July 23, 2007; In Final Form: October 24, 2007

A-type rotational spectra of the complex $HNO_3-(H_2O)_2$ have been observed by rotational spectroscopy in a supersonic jet. Extensive isotopic substitution and analysis of the resulting moments of inertia reveals that the complex adopts a cyclic geometry in which a second water inserts into the weak secondary hydrogen bond of the (also cyclic) HNO_3-H_2O dimer. The complex is planar, except for one free proton from each water unit that lies above or below the plane. The primary hydrogen bond, formed between the HNO_3 proton and the first water molecule in the trimer, is 1.643(76) Å in length. All intermolecular distances are smaller than those of the constituent dimers. Internal motion, inferred from spectral doubling and studied by isotopic substitution experiments, likely corresponds to proton interchange involving the second water unit, but no such motion is revealed by the a-type spectrum for the first water unit. The degree of proton transfer across the hydrogen bond is discussed in terms of the proton-transfer parameter, ρ_{PT}, which assesses the degree of ionization on the basis of interatomic distances. Measured in this way, the complex is best described as hydrogen bonded, in accord with numerous theoretical predictions. However, an increase in the degree of ionization relative to that in HNO_3-H_2O is discernible. Using ρ_{PT} as a metric, two water molecules do less to ionize nitric acid than one water does to ionize sulfuric acid.

Introduction

The chemistry of gas phase and crystalline hydrates of nitric acid has been an area of considerable interest for over two decades.[1−13] Nitric acid itself is a component of acid rain and plays a complex role in the chemistry of the atmosphere. Its crystalline hydrates, moreover, are famous for their role in polar stratospheric ozone depletion.[11,12] In the gas phase, molecular hydrates are of interest in relation to a variety of other atmospheric processes including nucleation, climate forcing, and photochemical activity of trace gases,[13−18] and from a fundamental perspective, the aggregation of water with HNO_3 provides an opportunity to investigate the relationship between hydration and ionization of a simple inorganic acid. Thus the study of the HNO_3-H_2O interaction is of interest from a number of different points of view.

Stable, hydrated forms of nitric acid were first identified and isolated as the mono- and trihydrates (NAM and NAT) in 1893 by freezing mixtures of HNO_3 and water.[19] Crystal structures of NAM and NAT were determined in the early 1950s,[20] and later to greater precision in 1975,[21,22] but the dihydrate (NAD) at the time, remained unknown. Indeed, the isolation and characterization of crystalline NAD lagged that of NAM and NAT by about a century. However, on the basis of much work including IR,[12,23,24] X-ray,[25,26] and calorimetric studies,[27,28] the existence of the dihydrate in two distinct, condensed/crystalline phases is now also firmly established.

Gas-phase nitric acid clusters and aerosols containing small molecules such as H_2O, NH_3, HCl, OH, and H_2SO_4 have been studied in the infrared,[29] microwave,[5,30] and ultraviolet spectral regions,[31] in aerosol chambers and flow cells,[32,33] by kinetic methods,[34] in fast flow reactors,[35] and with electrospray mass spectrometry.[36] Well-ordered and amorphous *crystalline* nitric acid hydrates in solid and small-particle form have also been studied with X-ray diffractometry,[20−22,37] and IR techniques.[38−40] Extensive work has been done with HNO_3, H_2O, HCl, and H_2SO_4 on surfaces in the form of thin films, with analysis by methods such as temperature programmed desorption, IR spectroscopy, and mass spectrometry.[23,24,41−44] Other methods of exploring nitric acid interactions with various species have been applied in argon matrices,[7,45−47] and as adsorbed aqueous systems on finely divided surfaces such as silica powder.[48] Theoretical work on isolated gaseous and crystalline complexes of nitric acid paired with a variety of chemical species have also been reported for over two decades.[3,4,6−8,10,49−57]

Several theoretical reports dealing with the structure and energetics of hydrated forms of HNO_3 existed in the literature prior to 1997,[3,50,58] and a number of systematic calculations of sequentially hydrated nitric acid have been reported since 2002.[7−10] The only experimental structural study of a gas-phase nitric acid hydrate to date, however, is for the monohydrate, HNO_3-H_2O.[5] Thus, in light of the broad interest in these systems, we present in this paper a gas-phase microwave study of the next higher hydrate of nitric acid, $HNO_3-(H_2O)_2$.

Experimental Section

Rotational spectra were recorded using a pulsed-nozzle Fourier transform microwave spectrometer which has been described elsewhere.[59] The $HNO_3-(H_2O)_2$ complex was produced with an injection source previously used in our laboratory for the study of reactive systems.[5,59−61] The parent isotopic species of the complex (as well as the previously studied monohydrate, HNO_3-H_2O[5]) could be observed by flowing

* Corresponding author. E-mail: kleopold@chem.umn.edu.
† Present address: Department of Chemistry Columbia University, New York, NY 10027.
‡ Present address: Jet Propulsion Laboratory, Pasadena, CA 91109.

10.1021/jp075789f CCC: $40.75
Published on Web 01/03/2008

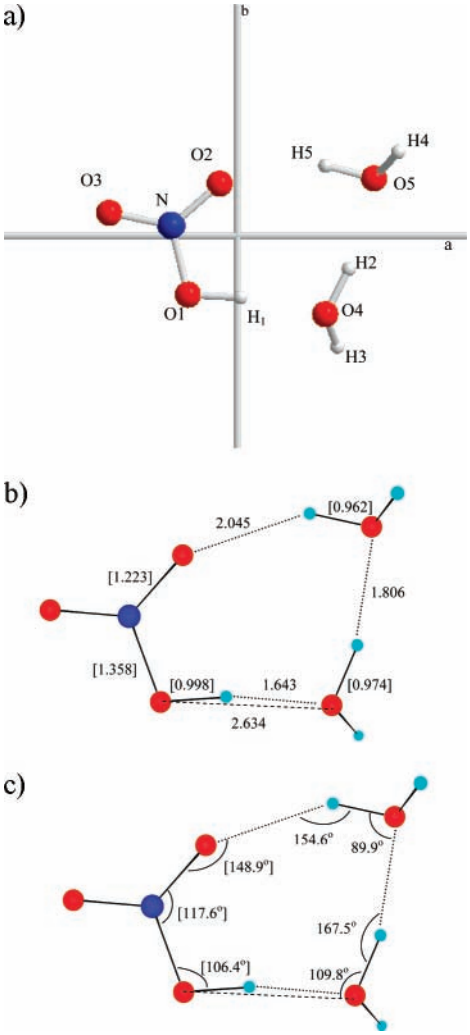

Figure 1. Three views of the $HNO_3-(H_2O)_2$ complex showing (a) atom numbering and orientation of the inertial axis system, (b) intermolecular bond distances, and (c) intermolecular bond angles. Values are those determined from the least-squares fit using distorted-monomer geometries as described in the text. Values in square brackets were held fixed in the fit.

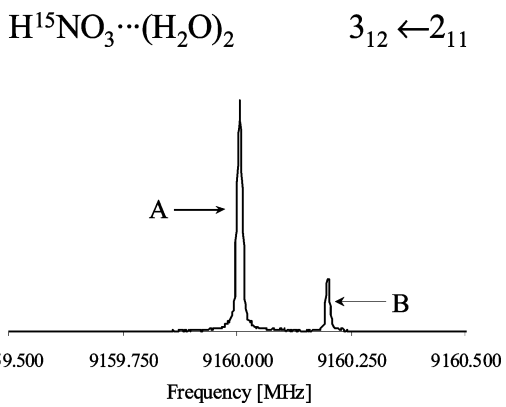

Figure 2. $3_{12} \leftarrow 2_{11}$ transition of $H^{15}NO_3-(H_2O)_2$ showing the spectral doubling, uncomplicated by ^{14}N nuclear hyperfine structure. This spectrum results from the average of 1800 free induction decays.

argon through a 90% aqueous solution of HNO_3, and expanding the resulting mixture. However, significantly better signals, up to 2 orders of magnitude more intense, were obtained by using the injection source to separately introduce water vapor into the early phases of an Ar/HNO_3 supersonic expansion. The water vapor in these experiments was entrained in a flowing stream of argon gas passed through a small glass bubbler. In some experiments, a mass flow controller (MKS model 1479A) was employed to regulate flow through the bubbler, with an optimum rate found to be about 5 standard cubic centimeters per minute (sccm). With a nozzle diameter of 0.8 mm, optimum stagnation pressures were in the range from 2.5 to 3 atm. The microwave pulse length used for observation of $HNO_3-(H_2O)_2$ signals was 1.7 μs and 5 free induction decays were recorded per gas pulse.

Rotational transitions of $HNO_3-(H_2O)_2$ were initially identified by the presence of ^{14}N nuclear quadrupole hyperfine structure and by their dependence on H_2O and HNO_3 in the expansion. In addition, select rotational transitions for two isotopic species (parent and $HNO_3-(D_2O)_2$) were tested to rule out the possibility of an argon-containing complex by using a 70% neon:30% helium mixture in place of argon as a carrier gas. Signal intensities were found to be lower using this carrier gas, but the transitions were clearly visible, confirming that the complex did not contain argon. Final confirmation of the identity of the complex was derived from ability to accurately predict the spectra of numerous isotopically substituted forms.

$H^{15}NO_3$ and DNO_3 were synthesized from $Na^{15}NO_3$ and concentrated H_2SO_4, or $NaNO_3$ and D_2SO_4, respectively, using previously reported procedures.[5,62] Mixed isotopic species involving substitution of the water units were formed by mixing H_2O and D_2O or $H_2{}^{18}O$, as appropriate, in various proportions in the water bubbler. Additional experimental details are given elsewhere.[63]

Results

Spectra. A-type rotational transitions of 18 isotopic forms of the nitric acid dihydrate complex were observed in this study. For eleven of these species, numerous rotational transitions were recorded, and for the remaining seven, all of which contained partially deuterated water units, only three or fewer rotational transitions were observed. However, based on good agreement between calculated and observed isotope shifts and dependence of signal intensities on H_2O/D_2O proportions in the water bubbler, the isotopic assignments are made with confidence. The estimated uncertainties in the measured frequencies for this work ranged from a few kHz up to ~15 kHz, depending on the degree of unresolved or partially resolved hyperfine structure for the D_2O- containing species. For many of the isotopic forms studied, the spectra appeared doubled, indicating the presence of a pair of states, which are arbitrarily labeled A and B. These states arise from internal motions of the complex and are discussed in greater detail below. Tables of transition frequencies for all observed species are provided as Supporting Information. In these tables, and throughout this paper, isotopic forms are designated by the mass numbers of the constituent atoms, using the atom numbering scheme shown in Figure 1a. A trace of the $3_{12} \leftarrow 2_{11}$ transition of the ^{15}N substituted species is presented in Figure 2. For this species, the spectrum is uncomplicated by nitrogen nuclear hyperfine structure and the separate spectra due to states A and B are particularly apparent.

All spectra were fit to the semirigid rotor Hamiltonian of eq 1.[64] Only two distortion constants, Δ_J and Δ_{JK}, were needed to

$$H = [(B+C)/2 - \Delta_J \mathbf{J}^2]\mathbf{J}^2 + [A - (B+C)/2 - \Delta_{JK}\mathbf{J}^2 - \Delta_K \mathbf{J}_z{}^2]\mathbf{J}_z{}^2 + [(B-C)/2 - 2\delta_J \mathbf{J}^2](\mathbf{J}_x{}^2 - \mathbf{J}_y{}^2) - \delta_K[\mathbf{J}_z{}^2(\mathbf{J}_x{}^2 - \mathbf{J}_y{}^2) + (\mathbf{J}_x{}^2 - \mathbf{J}_y{}^2)\mathbf{J}_z{}^2] \quad (1)$$

fit the data to within experimental uncertainty and hence Δ_K, δ_J, and δ_K were set to zero. Separate fits were done for the A

TABLE 1: Rotational and Hyperfine Constants[a] of $HNO_3-(H_2O)_2$[b]

N	H1	O4	H2	H3	O5	H4	H5	state	$A-(B+C)/2$	$(B+C)/2$	$(B-C)/2$	Δ_J	Δ_{JK}	χ_{aa}	$\chi_{bb}-\chi_{cc}$
14	1	16	1	1	16	1	1	A	3307.413(72)	1433.9684(4)	208.6238(4)	0.563(38)	3.71(25)	−0.8865(34)	0.5887(82)
14	1	16	1	1	16	1	1	B	3307.465(66)	1433.9875(4)	208.6520(4)	0.588(35)	3.45(22)	−0.8896(33)	0.5854(82)
14	2	16	1	1	16	1	1	A	3244.414(48)	1429.2936(5)	210.2410(6)	0.461(30)	3.74(26)	−0.9091(48)	0.628(12)
14	2	16	1	1	16	1	1	B	3244.325(63)	1429.3132(6)	210.2704(7)	0.396(35)	3.84(45)	−0.9265(71)	0.544(21)
15	1	16	1	1	16	1	1	A	3312.607(45)	1427.4932(8)	206.8354(7)	0.590(29)	3.79(10)		
15	1	16	1	1	16	1	1	B	3312.642(47)	1427.5123(7)	206.8642(8)	0.601(29)	3.75(10)		
14	1	16	2	1	16	1	1	A	3309.319(43)	1414.6693(6)	203.7980(4)	0.539(21)	3.71[c]	−0.8972(63)	0.628(22)
14	1	16	2	1	16	1	1	B	3309.199(45)	1414.6873(8)	203.8240(4)	0.496(27)	3.71[c]	−0.802(14)	0.504(16)
14	1	18	1	1	16	1	1	A	3156.19(14)	1405.6848(9)	208.3211(7)	0.419(60)	4.9(14)	−0.862(13)	0.575(30)
14	1	18	1	1	16	1	1	B	3155.67(19)	1405.7030(13)	208.3466(8)	0.173(69)	6.9(18)	−0.880(14)	0.608(43)
14	1	16	1	1	18	1	1	A	3266.450(86)	1377.7578(8)	196.8256(8)	0.487(46)	3.17(40)	−0.9027(87)	0.608(26)
14	1	16	1	1	18	1	1	B	3266.322(97)	1377.7726(11)	196.8506(7)	0.467(61)	3.10(35)	−0.926(15)	0.770(88)
14	1	18	1	1	18	1	1	A	3103.594(94)	1353.2650(5)	197.8188(5)	0.473(50)	3.36(28)	−0.8880(49)	0.5885(98)
14	1	18	1	1	18	1	1	B	3103.437(99)	1353.2809(6)	197.8432(6)	0.480(53)	3.48(30)	−0.8825(55)	0.678(14)
14	1	16	1	1	16	1	2	A	3230.297(45)	1421.2264(10)	208.7583(5)	0.500(34)	3.71[c]	−0.891(45)	0.582(64)
14	1	16	2	1	16	1	2	A	3230.314(83)	1402.5204(11)	204.1330(10)	0.587(44)	3.71[c]	−0.951(17)	0.43(12)
14	1	16	2	2	16	1	2	A	3064.635(54)	1380.8831(7)	204.7209(6)	0.447(32)	3.71[c]	−0.905(11)	0.88(12)
14	1	16	2	2	16	2	2	A	2990.945(45)	1343.1210(6)	197.6527(6)	0.410(25)	3.71[c]	−0.8831(55)	0.567(22)

[a] All values in MHz, except for Δ_J, Δ_{JK} which are in kHz. Numbers in parentheses represent uncertainty in the last digit and are one standard error from the least-squares fit. [b] Isotopic species are indicated by atomic mass numbers according to the atom numbering scheme of Figure 1a. Only atoms which were isotopically substituted in this study are listed. [c] Held fixed to value of parent isotopic species.

and B states, when observed. Fitted values of the spectroscopic constants for the eleven most thoroughly studied derivatives are given in Table 1 and residuals from the fits, which were generally within the experimental uncertainties, are included in the Supporting Information.

B-type rotational transitions were not assigned in this work. Although the A rotational constant is reasonably well determined from the a-type spectra (Ray's asymmetry parameter, $\kappa = -0.76$ for the parent species), spectral searches in the vicinity of the predicted b-type lines failed to produce results. However, acknowledging the possibility that the desired spectra could be perturbed by internal motions, a broader series of searches was conducted in the vicinity of each of four predicted b-type transition frequencies for the parent complex. These revealed four sets of transitions, each within 10−50 MHz of a predicted frequency, but no subgroup of these could be fit together with the assigned a-type spectra. Moreover, only some displayed what appeared to be nitrogen hyperfine structure, and even for these, the splittings were not commensurate with predictions based of the hyperfine parameters determined from the a-type lines. Further searches for several deuterated and partially deuterated species, for which the effects of internal motion should be reduced, were also conducted but were similarly unsuccessful.[65]

At the Hartree−Fock level of theory, the dipole moment projection for the complex is 12 to 13 times smaller along the b-principal axis than along the *a*-axis.[67] Thus, it seems likely that the desired b-type transitions were too weak to observe and that the lines described above arise from some other cluster in the supersonic jet. Of course it is possible that the transitions recorded are indeed the desired b-type spectra, perturbed in a way that is at present not understood. However, we note in this regard that internal motions in the cyclic trimers $HCl-(H_2O)_2$[66a] and $HBr-(H_2O)_2$[66b] produced a simple quadrupling of the b-type spectra of those species, quite unlike the spectral patterns observed here. Fortunately, the a-type spectra and the extensive isotopic substitution are sufficient for the elucidation of the structure of the complex. A detailed account of our efforts to observed b-type transitions may be found elsewhere.[63] Although a small value for the dipole moment component along the c-inertial axis is also expected, no searches for c-type transitions were conducted.

Internal Dynamics. As noted above, for many isotopic forms of the complex the a-type spectra appeared doubled, presumably due to a pair of states which have been labeled A and B. For any given isotopic derivative, the magnitude of the splitting between the A and B state spectra was dependent on the rotational transition and ranged from about 25−200 kHz. Relative intensities were not accurately measured but did appear to vary according to rotational transition, ranging, for example, from about 4:1 to 7:1 for the A:B state ratio intensity of $H^{15}NO_3-(H_2O)_2$. Because relative intensities can depend sensitively on a variety of factors, including the offset between the molecular transition frequency and the cavity frequency, variations of this magnitude are not uncommon and reliable intensities can be difficult to obtain.

The spectral splittings observed here are reminiscent of those common to water complexes and to those previously reported for the closely related systems HNO_3-H_2O[5], $HCl-(H_2O)_2$,[66a] and $HBr-(H_2O)_2$.[66b] In HNO_3-H_2O, both the a-type and b-type spectra were doubled, with isotopic substitution experiments indicating a proton interchange motion involving equivalent protons on the H_2O moiety. A wagging of the free water hydrogen above and below the heavy atom plane was also inferred from the absence of rigid rotor c-type transitions. For the cyclic trimers $HCl-(H_2O)_2$ and $HBr-(H_2O)_2$, each with two waters present, the a-type spectra also appeared as doublets, but the b-type spectra were quadrupled (i.e, formed doublets of doublets). The presence of four states (labeled S, S′, W, and W′) was inferred for these systems, and the doubling of the a-type spectra was interpreted as a collapse of one pair of doublets beneath the limits of resolution. It is entirely reasonable that such a situation pertains for $HNO_3-(H_2O)_2$ as well, but in absence of observable b-type transitions, such a scenario remains only a plausible hypothesis.

Isotopic substitution experiments shed light on the internal motion within the complex. As in the related systems, the obvious candidates for water motion are (i) interchange of the roles of the free and bound water protons on either or both of the waters and (ii) wagging of the free water protons above and below the heavy atom plane. Careful examination of the spectra, and of the isotopic dependence of $(B+C)/2$ and $(B-C)/2$ for the A and B states of the complex, reveals that substitution on the first water (H2−O4−H3) has no effect, whereas substitution on the second water (H4−O5−H5) either alters the magnitude of the splitting or causes it to disappear entirely. In particular, we observe that two states are observed

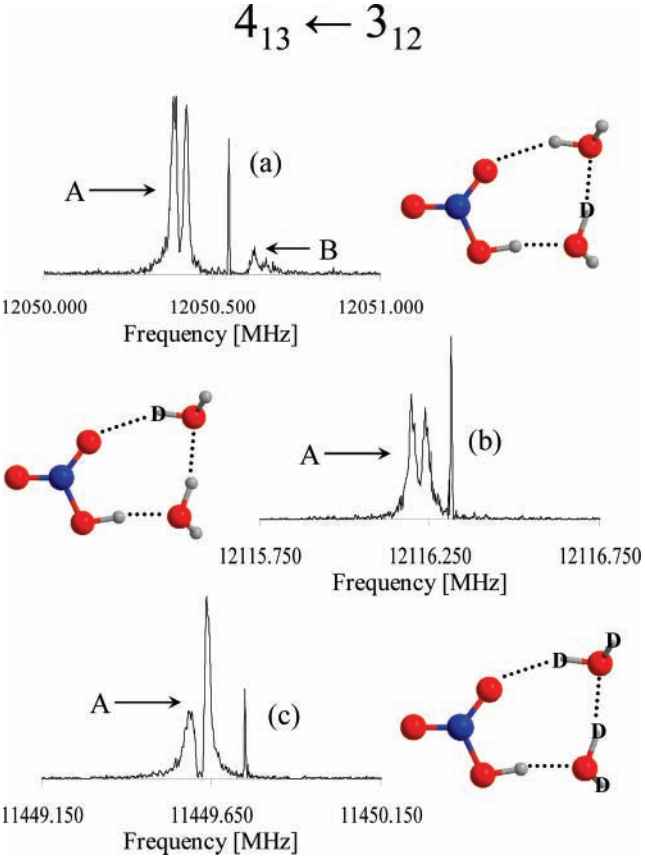

Figure 3. $4_{13} \leftarrow 3_{12}$ transition in several deuterated forms of $HNO_3-(H_2O)_2$. (a) Deuterium in hydrogen-bonding position of first water unit. (b) Deuterium in the hydrogen-bonding position of the second water unit. (c) Fully deuterated water units. The narrow spike in the middle of each spectrum marks the cavity frequency and is not a part of the rotational spectrum. (a)−(c) are the result of 18 000, 12 000, and 12 000 free induction decays, respectively. The multiple peaks in the "A" state transition in (a)−(c) and the "B" state transition of (a) are ^{14}N nuclear hyperfine structure.

for the D2 substituted form, and that the A/B state difference for $(B + C)/2$ and $(B - C)/2$ is the same for that species as that observed in the parent and $^{18}O4$ substituted forms (see Table 1). This point is further illustrated in Figure 3, which shows the $4_{13} \leftarrow 3_{12}$ transition for three isotopic species having full or partial deuteration on the water moieties. Figure 3a, corresponding to deuterium in the hydrogen-bonding position on the first water unit (D2), shows the presence of two transitions (each split by ^{14}N hyperfine structure), corresponding to the two states A and B. If the observed doubling involved an exchange motion between the bound and free hydrogens of the first water, the inequivalency of the hydrogens of the HOD would quench the tunneling and eliminate the spectral splitting. That the splitting persists for this isotopic form, therefore, indicates that the causative motion does not involve hydrogen exchange on the first water unit.

In contrast, Figure 3b shows the same rotational transition for the species with deuterium in the hydrogen-bonded position of the second water (D5) and clearly shows the disappearance of the A/B state spectral doubling. We note, in this regard, that the spectrum in Figure 3b is more intense than that in Figure 3a and thus the second state, if present, should have been observable. Also, though not shown in the figure, ^{18}O substitution in the O5 position was found to slightly reduce the difference in A and B state rotational constants relative to the parent form but did not cause the disappearance of the second state. The sensitive dependence of the spectral doubling to isotopic substitution on the second water is a clear indicator that the observed motion primarily involves that moiety, and its disappearance in the case of the HOD species strongly suggests an exchange motion between the bound and free hydrogens.

Figure 3c shows the same transition for the complex with full deuteration on the water and once again, the B state spectrum is absent. Although all deuteriums are equivalent in this case, and deuterium interchange is, in principle possible, it is entirely reasonable that the increased mass of deuterium could quench such a motion, thus reducing the splitting below the observed line width (which is, itself, larger than that of the parent species due to the presence of four quadrupolar deuterium nuclei).

In general, for $HNO_3-(H_2O)_2$, mixed deuterated (HOD) isotopic species exhibited more intense spectral signals when deuterium was in the hydrogen-bonding position, though some transitions arising from species with deuterium in the non-hydrogen-bonded position were also observed. These intensities are consistent with observation[5] and theory[68] that deuterium shows a preference for occupying hydrogen-bonding positions in neutral water complexes.

In summary, isotopic substitution experiments indicate that the internal motion responsible for the observed doubling of the a-type spectrum of $HNO_3-(H_2O)_2$ likely arises from a motion involving bound−free hydrogen interchange on the second water unit (H4−O5−H5). Spectral features signaling a similar motion on the first water are not observed, though the existence of additional motion not revealed by the a-type spectrum cannot be ruled out. It should be noted that the arguments above do not preclude the possibility of wagging-type motions of either or both of the free hydrogens, but the present data do not allow additional conclusions to be drawn with certainty.

Structure Determination

Analysis of Rotational Constants. Preliminary analysis of the measured rotational constants was consistent with a model in which the heavy-atom structure of $HNO_3-(H_2O)_2$ is planar, in accord with *ab initio* calculations.[7,8,10] The HNO_3 and H_2O units are oriented in a cyclic fashion to form an eight-membered ring, as shown in Figure 1. The inertial defect for 8 of the 11 primary isotopologues studied is small in magnitude, close to -1.8 amu·Å^2, and those for the three other more extensively deuterated water species are, as expected, slightly larger in magnitude (-1.9 to -3.4 amu·Å^2). In all cases, the inertial defects calculated from the observed rotational constants are smaller than those for the *ab initio* structure. On this basis, and in light of the *ab initio* results, the heavy atom ring is constrained to be planar in the analysis which follows.

The rotational constants given in Table 1 were used to determine the structure of $HNO_3-(H_2O)_2$ in three different ways: (i) nonlinear least-squares fitting to intermolecular coordinates assuming the individual monomers undergo *no* structural changes upon complexation, (ii) least-squares fitting to intermolecular coordinates using monomer structures derived by imposing the *ab initio* changes upon complexation[7] onto experimental geometries,[69,70] and (iii) a Kraitchman[71] analysis.

Least-squares fits were performed using the program STRFIT described by Kisiel.[72] Because STRFIT uses coordinates entered from a **Z**-matrix, and because the construction of the **Z**-matrix is not unique, several sets of coordinates were tried. These gave generally excellent agreement, and therefore only one is presented here. Additional information may be found else-

TABLE 2: Structural Parameters for $HNO_3-(H_2O)_2$

	least-squares fitting[b]			
parameter[a]	undistorted monomers[d]	distorted monomers[e]	Kraitchman	ab initio[c]
r(O4−N)			3.339	3.3864
r(O4−O1)	2.612(17)	2.634(16)		2.6330
r(H2−O4)			1.014	0.9829
r(O5−O4)	2.758(11)	2.765(11)	2.745	2.7370
r(O5−N)			3.953	3.9547
r(H5−N)			3.064	3.1729
r(H5−O5)			1.119	0.9709
a(N−O1−O4)				111.7
a(O1−O4−H2)	110.6(28)	109.8(25)		112.5
a(O5−O4−O1)	102.17(55)	101.65(51)		101.7
a(O5−N−O4)			43.2	42.9
a(H4−O5−O4)	137.9(59)	136.7(55)		127.2
a(H5−O5−O4)			88.3	89.2
τ(H3−O4−H2−N)	122.5(48)	122.2(45)		126.0
τ(H4−O5−O4−N)	107.2(56)	108.2(52)		111.8
τ(H5−O5−H4−N)	22.2(59)	23.8(52)		27.8
Ring Parameters from Cartesian Coordinates[f]				
r(O1−H1)	[0.964]	[0.998]		1.0109
r(H1−O4)	1.669	1.643(76)		1.6294
r(O4−H2)	[0.9565]	[0.9735]		0.9829
r(H2−O5)	1.818	1.806(15)		1.7809
r(O5−H5)	[0.9565]	[0.9615]		0.9709
r(H5−O2)	2.044	2.045(52)		2.0482
r(O2−N)	[1.211]	[1.223]		1.2338
r(N−O1)	[1.406]	[1.358]		1.3681
a(N−O1−H1)	[102.15]	[106.4]		106.3
a(O1−O4−H2)	110.6	109.8(51)		112.5
a(O4−H2−O5)	167.1	167.5(50)		163.3
a(H2−O5−H5)	89.7	89.9(50)		95.1
a(O5−H5−O2)	154.9	154.6(57)		149.9
a((H5−O2−N)	150.1	148.9(82)		149.4
a(O2−N−O1)	[115.88]	[117.6]		117.6

[a] "*r*" represent the distance, in Å, between indicated atoms. "*a*" represents the angle, in degrees, between indicated atoms. "*τ*" represents the dihedral angle, in degrees, between indicated atoms. [b] Values from least-squares fitting using STRFIT. Uncertainties are one standard error in the fit. [c] Values derived from the MP2/aug-cc-pVDZ calculations of ref 7. [d] Values from fits using experimental free-monomer geometries. Values in square brackets were held fixed in the fit. [e] Values from fits using experimental free-monomer geometries corrected using the *ab initio*-calculated distortions upon complexation. These values are preferred over those using undistorted-monomer geometries. Values in square brackets were held fixed in the fit. [f] Calculated from atomic Cartesian coordinates generated from least-squares fitting. See text for discussion of uncertainties.

where.[63] In the definition of coordinates used here, the heavy atoms, as well as the bound hydrogen of the first water (H2) were constrained to lie in a plane, whereas the O5−H5 bond was not. Further constraint of the O5−H5 bond to the plane was tried in other trial fits but had a negligible effect on the results. Experimental geometries for HNO_3 and H_2O were taken from refs 69 and 70, respectively, and the changes in structure upon complexation were obtained from atomic Cartesian coordinates provided to us by Xantheas.[67] Structural parameters arising from fits using both free-monomer and distorted-monomer geometries are given in the top half of Table 2. These results show that changes in monomer geometries upon complexation have a relatively small effect on the fitted structure of the complex. Thus, the imposition of changes in monomer structures upon complexation amounts only to a small correction, and because the results are likely to be more accurate with this correction than without it, we regard structural parameters derived from "distorted-monomer" fits as preferred over those employing the unperturbed monomer geometries.

TABLE 3: Atomic Cartesian Coordinates in the Inertial Axis System for $HNO_3-(H_2O)_2$ Derived from a Least-Squares Fit Using Distorted-Monomer Geometries

atom	*a* [Å]	*b* [Å]	*c* [Å]
O1	−0.9478	−1.1259	0.0553
N	−1.2592	0.1945	−0.0044
O2	−0.3341	0.9936	−0.0430
O3	−2.4376	0.4459	−0.0132
H1	0.0487	−1.1807	0.0556
O4	1.6575	−1.5126	0.0671
H2	2.1182	−0.6560	0.0268
H3	1.9544	−2.0219	−0.6861
O5	2.6073	1.0809	−0.0538
H4	3.0405	1.6918	0.5411
H5	1.6814	1.3393	−0.0735

Although the parameters resulting from the above fits were generally well determined, we observed a strong correlation between the O1−O4 distance and the N−O1−O4 angle. For this reason, several additional fits were performed with the N−O1−O4 angle held fixed at a series of values. As expected, most of the fitted structural parameters were relatively insensitive to the value chosen, but the O1−O4 distance was notably affected. For those angles which are not strongly affected by this correlation, the agreement with *ab initio* calculations is quite good, typically within a few degrees. Thus, it is reasonable to assume that the *ab initio* value for the N−O1−O4 angle is also accurate within a few degrees and the results in the top half of Table 2 are those obtained by holding this angle fixed at the *ab initio* value (111.7°). Uncertainties associated with this constraint are discussed later in this section.

The particular construction of the **Z**-matrix indicated by the parameters in Table 2 is convenient for performing the fits using STRFIT but does not produce distances and angles that are intuitive from the point of view of understanding the intermolecular degrees of freedom. With the structure uniquely specified, however, atomic Cartesian coordinates are produced and these are readily used to calculate intermolecular structural parameters. A table of atomic Cartesian coordinates arising from the distorted-monomer fit is given in Table 3. The important intermolecular structural parameters calculated from them are given in the lower portion of Table 2 and are shown in Figure 1b,c. Also included (in square brackets) are some of the monomer bond lengths and distances that were held fixed in the fit, but which form part of the eight member ring. It should be noted that the acidic proton of the HNO_3 is directly on the b-principal axis in the *ab initio* structure[7,67] (see Figure 1a), and thus, determining its location with isotopic substitution by deuterium proved difficult. Indeed, this isotopic substitution was the only one found to produce an experimental isotope shift appreciably different from that predicted by the *ab initio* structure, and the position of this atom proved impossible to realistically determine either by Kraitchman analysis or by least-squares fitting. Moreover, it seems likely that the position of this atom in the inertial axis system is at the root of the correlation between *r*(O1−O4) and *a*(O4−O1−N): Although ^{15}N substitution, in effect, determines the distance between HNO_3 and the $(H_2O)_2$ unit, another substitution on the HNO_3 is needed to determine its orientation. With substitution on H1 only marginally helpful, ^{18}O substitution on the HNO_3 may be what is needed to decorrelate these parameters. The cost of obtaining ^{18}O substituted nitric acid, however, was deemed prohibitive, and we therefore settle for somewhat larger uncertainties on the H1−O4 distance, as discussed below.

For most of the important intermolecular structural parameters, the largest source of uncertainty arises from the choice

of the O4−O1−N angle. To assess the magnitude of this uncertainty, the following procedure was adopted: In view of the observation, noted above, that *ab initio* calculations give ring angles that are accurate to within a few degrees, additional fits using the distorted-monomer geometries were run with the O4−O1−N angle fixed at ±5° about the *ab initio* value of 111.7°. The resulting atomic coordinates were again used to calculate intermolecular distances and angles, and the variation in values was taken as the uncertainty associated with the use of the *ab initio* O4−O1−N angle. Note that uncertainties determined in this way do not include the standard errors resulting from the least-squares fits themselves because the least-squares fits employed different parameters (defined by the **Z**-matrix). The standard errors in the least-squares fits (top portion of Table 2) are seen to be typically a 0.01−0.02 Å for distances and about 5° for angles. Thus, the uncertainties quoted in the lower portion of Table 2 were derived by combining those associated with the use of the *ab initio* O4−O1−N angle with 0.015 Å for distances and 5° for angles.

The last column of Table 2 gives the structural parameters derived from *ab initio* theory,[7] and the overall agreement is seen to be quite good. It is interesting to note that the angles for the non-hydrogen-bonded water protons were allowed to float in least-squares structure fits and the agreement between the experimentally determined and *ab initio* calculated angles is remarkable. Significant large amplitude internal motion likely takes place for these water units, however, so the agreement may be fortuitous. The final reported structure has H3 in the "down" and H4 in the "up" position, looking down at the trimer in the *a*−*b* plane. Additional fits were performed with both out-of-plane hydrogens on the same side of the heavy atom plane. These fits converged well (both hydrogen atoms remaining on one side of the heavy atom plane) and gave virtually identical results for all heavy atom distances and angles as the fits with these hydrogen atoms in an up/down orientation, indicating the observed spectra are not sensitive to this aspect of the structure. Despite the likely presence of internal motion, isotope shifts for deuterated water units were within 10 MHz of those predicted by calculations and the structure fits exhibited no major convergence problems as long as the water monomer bond lengths were held fixed.

Structural information obtained from the Kraitchman analysis is also included in Table 2. The results are in good agreement with the least-squares analysis for structural parameters that may be compared directly.

Analysis of Nuclear Quadrupole Coupling Constants. As an additional check of the structure, the angular orientation of the HNO_3 within the complex was investigated on the basis of the measured ^{14}N nuclear quadrupole coupling constants. Because the values of χ_{aa} and $\chi_{bb} - \chi_{cc}$ given in Table 1 represent projections of the HNO_3 coupling tensor onto the inertial axis system of the complex, structural information is, in principle, available from them provided the HNO_3 undergoes negligible electronic perturbation upon complexation. This assumption, of course, is not necessarily appropriate for $HNO_3-(H_2O)_2$ in light of the small but finite changes in the HNO_3 geometry within the complex calculated from *ab initio* theory. Nonetheless, the analysis was performed to see how close the results came to those obtained from rotational constants.

The *X*-axis of the principal axis system of the quadrupole coupling tensor of free HNO_3 (*X*, *Y*, *Z*) lies about 2° off the N−O(H) bond, tilted away from the hydrogen.[73,74] Thus, using the structure fitted above and the results of Ott et al.,[74] the X axis of HNO_3 and the a-inertial axis of the complex form an angle $\phi = 78.6°$. Ott et al. have reported the in-plane eigenvalues of the HNO_3 quadrupole coupling tensor to be $\chi_{XX} = 1.1468(34)$ MHz and $\chi_{YY} = -1.0675(34)$ MHz. Assuming that the *c*-axis of $HNO_3-(H_2O)_2$ is parallel to the *c*-axis of HNO_3 (i.e., that the plane of the complex is the plane of the HNO_3), these may be projected onto the inertial axis system of the complex by rotation, giving χ_{aa} and $(\chi_{bb} - \chi_{cc})$ as functions of ϕ:

$$\chi_{aa} = \chi_{XX}\cos^2\phi + \chi_{YY}\sin^2\phi \quad (2)$$

$$(\chi_{bb} - \chi_{cc}) = \chi_{XX}(1 + \sin^2\phi) + \chi_{YY}(1 + \cos^2\phi) \quad (3)$$

Because the *c*-axis of the complex forms an angle of only 2.6° with a vector perpendicular to the HNO_3 plane, this should be a reasonably accurate approximation. Using $\chi_{aa} = -0.8865$ MHz from Table 1 and solving eq 2 gives $\phi = 73.4°$, which is in remarkable agreement with the 78.6° value above. The agreement is deceptive, however, because the experimental value of $\chi_{bb} - \chi_{cc} = 0.5887$ MHz gives a value of ϕ of only 57.6° using eq 3. This discrepancy may be restated in terms of the variability of χ_{cc}: As noted above, the transformation between the principal axis system of the HNO_3 quadrupole coupling tensor and the inertial axis system of the complex axis corresponds closely to a rotation about an axis perpendicular to the HNO_3 plane. Thus, if the eigenvalues of the quadrupole coupling tensor of HNO_3 are truly unchanged upon complexation, χ_{cc} for the complex should equal χ_{ZZ} for free HNO_3. This expectation is not well fulfilled, however, as $\chi_{cc} = -{}^1/_2[\chi_{aa} + (\chi_{bb} - \chi_{cc})] = 0.1489(45)$ MHz, whereas $\chi_{ZZ} = -(\chi_{XX} + \chi_{YY}) = -0.0793(48)$ MHz for free HNO_3. Thus, it seems likely that there is some discernible change in the HNO_3 electronic structure upon complexation. As a result, the agreement between ϕ calculated from rotational constants and from quadrupole coupling data is probably about as good as can be expected. The structural information obtained from rotational constants, therefore, is expected to be superior to that obtained from quadrupole coupling data, and further analysis of the quadrupole coupling constants was not pursued.

Discussion

The excellent agreement between the experimentally determined structure and the *ab initio* results is very satisfying and indicative of a high level of confidence that can be placed in the results given in Table 2. The trimer adopts a cyclic geometry in which the second water unit inserts into the weak secondary hydrogen bond of HNO_3-H_2O. As noted above, the data do not determine whether the free water protons are on the same side or on opposite sides of the heavy atom plane. Apart from this, however, agreement between theory and experiment is quite reasonable, not only for interatomic distances but also for planar and dihedral angles between heavy atoms and H_2O protons as well. Intermolecular bond lengths, for example, match the theoretical values to within a few hundredths of an angstrom and bond angles are typically in agreement to within 5°. Some water OH distances were even determined from experimental data with the Kraitchman analysis and these results are also included in Table 2. Their differences from the experimental H_2O monomer structure seem a bit large but are not entirely unreasonable and are included for completeness.

Though not immediately obvious from the table, a distinctive feature of the trimer is that all intermolecular distances are contracted relative to those in the constituent dimers. Most important, perhaps, is that between the HNO_3 proton and the first water (H3−O4−H2). The O1−O4 distance in HNO_3-

$(H_2O)_2$ is 2.634(16) Å and, taking into account the O1−H1 distance and orientation in the HNO_3 moiety results in a very short hydrogen bond distance of 1.643(76) Å. It should be noted that this, in some sense, represents a "hybrid" value, as it involves both the experimental heavy atom distance and the OH bond length of nitric acid, corrected by imposing the theoretical elongation of 0.034 Å. Nonetheless, the correction is relatively small and the value obtained represents a contraction of 0.14(11) Å relative to the hydrogen bond distance in HNO_3−H_2O.[5]

The $(H_2O)_2$ moiety is similarly contracted relative to that in the free water dimer. In particular, the O4−O5 distance of 2.765(11) Å in the trimer represents a 0.22(2) Å contraction relative to that observed in $(H_2O)_2$.[75] The secondary hydrogen bond to HNO_3 is also substantially shorter in HNO_3−$(H_2O)_2$ than in HNO_3−H_2O: The H5−O2 distance derived from fitted parameters is 2.045(52) Å, which is 0.26 Å shorter than the analogous distance of 2.30 Å found for HNO_3−H_2O.

One of the goals of studying nitric acid hydrates is to assess the influence of sequential hydration on proton transfer across the hydrogen bond. Although numerous criteria have been applied to quantify the degree of ionization in hydrogen-bonded complexes, the results presented here are particularly amenable to the structural method given by Kurnig and Scheiner[76] and used previously in our laboratory for amine−hydrogen halide complexes.[61,77] Specifically, the proton-transfer parameter, ρ_{PT}, incorporates both shortening of the hydrogen bond and the elongation of the covalent OH bond of the acid to measure the extent of proton transfer, viz.,

$$\rho_{PT} = (r_{OH} - r^{\circ}_{OH}) - (r_{H\cdots O} - r^{\circ}_{H\cdots O}) \qquad (4)$$

where r_{OH} and r°_{OH} are the O−H distances in HNO_3 within the complex and the free monomer, respectively, and $r_{H\cdots O}$ and $r^{\circ}_{H\cdots O}$ are the hydrogen bond distances in $HNO_3\cdots(H_2O)_2$ and the H−O distance in fully protonated water (hydronium ion, H_3O^+), respectively. For a hydrogen-bonded complex, the first term is approximately zero and ρ_{PT} is negative. For a complex in which the proton is fully transferred to the water, the second term is zero and ρ_{PT} is positive. A value of ρ_{PT} near zero indicates equal proton sharing between the acid and the base. In terms of the parameters in Table 2, $r_{OH} = r$(O1−H1) and $r_{H\cdots O} = r$(H1−O4).

Using the H1−O4 distance of 1.643 Å in HNO_3−$(H_2O)_2$, we find $\rho_{PT} = -0.64$ Å. This value is, again, somewhat hybrid in that it utilities both experimental and theoretical distances. However, its magnitude is dominated by the experimental hydrogen bond lengths. The first term, for instance, is entirely theoretical and has a value of only 0.021 Å. In the second term, on the other hand, which has a value of −0.66 Å and therefore dominates ρ_{PT}, is largely experimental, combining the (predominantly) experimental hydrogen bond distance of the trimer with the experimental r_o value for H_3O^+ determined by Sears et al.[78]

The negative value of ρ_{PT} confirms the conclusions of many other studies, namely that two water molecules are insufficient to ionize nitric acid, at least in a cold molecular cluster. Indeed, there appears to be a consensus in the literature[7,8,10] that at least four water molecules are needed before a solvated ion pair appears as a local minimum on the potential energy surface for gas-phase complexes. In experimental studies, infrared spectra of submicron-sized particles have shown evidence of nitric acid ionization,[29] as does the solid, crystalline dihydrate itself.[25] This is to be expected, of course, as a multitude of near-neighbor interactions in a condensed environment are available to stabilize the ion pair with respect to recombination.

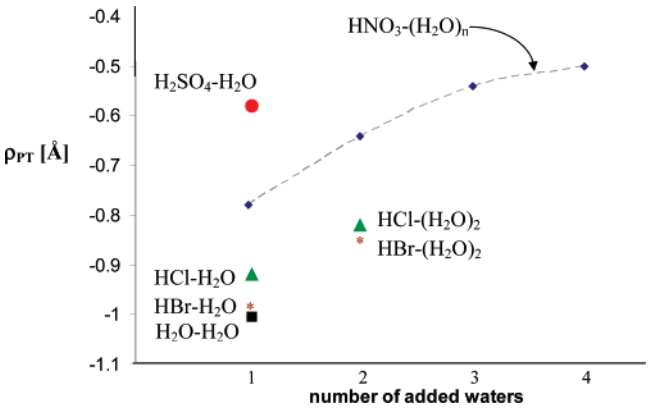

Figure 4. ρ_{PT}, in Å, for M−$(H_2O)_n$ vs n for several nitric acid hydrates, and other acidic hydrates. Diamonds correspond to M = HNO_3 and are connected by a dotted line for ease of viewing. $(H_2O)_2$ (■) is included as a reference point. Values of ρ_{PT} for HCl complexes (▲) and HBr complexes (*) were calculated from the literature. See text for discussion.

Although the complex is certainly best described as hydrogen bonded, the calculation of ρ_{PT} provides a means of tracking the system's progress toward ionization and of comparing that progress with that of other acids. For example, the value of ρ_{PT} calculated from our previously reported structure of HNO_3−H_2O is −0.78 Å. Thus, the addition of the second water of HNO_3−H_2O produces an increase in ρ_{PT} of about 0.14 Å relative to HNO_3−H_2O. A broader view of this change is presented in Figure 4, which plots ρ_{PT} for HNO_3−$(H_2O)_n$ (n = 1−4). For n = 1 and 2, the experimental results are used, and for n = 3 and 4, the values are calculated from the *ab initio* structures. A value for $(H_2O)_2$,[79] in which proton transfer is assumed to be virtually absent, is plotted as a reference species. Also included is a value of ρ_{PT} obtained from our previously published structure of H_2SO_4−H_2O,[80] as well as those of HCl−H_2O,[81] HBr−H_2O,[82] and the cyclic trimers HCl−$(H_2O)_2$ and HBr−$(H_2O)_2$ reported by Kisiel and co-workers.[66,83] It is interesting to note that, to the extent that ρ_{PT} is a good measure of proton transfer, two water molecules do less to ionize HNO_3 than one water molecule does to ionize H_2SO_4. This is consistent with the smaller proton affinity of HSO_4^- (−1312 kJ/mol) relative to NO_3^- (−1357 kJ/mol).[84] HCl fits smoothly in this series, with PA(Cl^-) = −1394.9 kJ/mol, but HBr does not (PA(Br^-) = −1353.5 kJ/mol). In any case, HCl and HBr appear less apt to release their proton to water in this cluster size regime.

Conclusion

Key results of this study are summarized as follows:

1. Microwave spectroscopic studies indicate that the geometry of HNO_3−$(H_2O)_2$ is cyclic with the heavy atoms lying in a plane, and that the second H_2O molecule inserts into the secondary hydrogen bond of HNO_3−H_2O. The near-linear hydrogen bond formed between the acidic proton of the HNO_3 and the first water oxygen is quite short, only 1.643(76) Å in length. There are successively longer hydrogen bonding interactions of 1.806(15) and 2.045(52) Å between the first and second water units and the second water unit and the oxygen (O2) of the nitric acid, respectively.

2. The addition of a second water molecule to HNO_3−H_2O has a significant effect on the structure of the nitric acid monohydrate. All intermolecular distances in HNO_3−$(H_2O)_2$ are contracted relative to those in HNO_3−H_2O and $(H_2O)_2$.

3. Observed rotational spectra indicate internal motion within the complex. Isotopic substitution experiments indicate that the motion observed primarily involves the second water unit, which is presumably more weakly bound. It is possible that additional motions may be present that are not revealed in the observed a-type spectrum.

4. Using the proton-transfer parameter, ρ_{PT}, to measure the extent of proton transfer, we find that the addition of the second water unit produces a measurable increase in the degree of proton transfer. However, the complex is still best described as hydrogen bonded. As measured by ρ_{PT}, two water molecules do less to ionize HNO_3 than one water molecule does to ionize H_2SO_4.

Acknowledgment. We thank Dr. Sotiris S. Xantheas for kindly providing Cartesian coordinate output of geometry optimizations and binding energy calculations for nitric acid dihydrate in the early stages of this project. This work was supported by the National Science Foundation, grants CHE 0514256 and CHE 0132584. We are also grateful to Mr. M. C. Orilall for his synthesis of DNO_3.

Supporting Information Available: Tables of observed microwave frequencies, assignments, and residuals from the least-squares fits. This material is available free of charge via the Internet at http://pubs.acs.org.

References and Notes

(1) Włodek, S.; Łuczyński, Z.; Wincel, H. *Int. J. Mass Spectrom. Ion Phys*. **1980**, *35*, 39.
(2) Kay, B. D.; Hermann, V.; Castleman, A. W., Jr. *Chem. Phys. Lett*. **1981**, *80*, 469.
(3) Tao, F.- M.; Higgins, K.; Klemperer, W.; Nelson, D. D. *Geophys. Res. Lett*. **1996**, *23*, 1797.
(4) Nguyen, M.-T.; Jamka, A. J.; Cazar, R. A.; Tao, F.-M. *J. Chem. Phys*. **1997**, *106*, 8710.
(5) Canagaratna, M.; Phillips, J. A.; Ott, M. E.; Leopold, K. R. *J. Phys. Chem. A* **1998**, *102*, 1489.
(6) Gleitsmann, G.; Zellner, R. *Phys. Chem. Chem. Phys*. **1999**, *1*, 5503.
(7) McCurdy, P. R.; Hess, W. P.; Xantheas, S. S. *J. Phys. Chem. A* **2002**, *106*, 7628.
(8) Escribano, R.; Couceiro, M.; Gómez, P. C.; Carrasco, E.; Moreno, M. A.; Herrero, V. J. *J. Phys. Chem. A* **2003**, *107*, 651.
(9) D'Auria, R.; Turco, R. P.; Houk, K. N. *J. Phys. Chem. A* **2004**, *108*, 3756.
(10) Scott, J. R.; Wright, J. B. *J. Phys. Chem. A* **2004**, *108*, 10578.
(11) Solomon, S. *Rev. Geophys*. **1999**, *37*, 275 and references therein.
(12) Worsnop, D. R.; Fox, L. E.; Zahniser, M. S.; Wofsy, S. C. *Science* **1993**, *259*, 71.
(13) Vaida, V.; Kjaergaard, H. G.; Feierabend, K. J. *Int. Rev. Phys. Chem*. **2003**, *22*, 203.
(14) Frost, G. J.; Vaida, V. *J. Geophys. Res*. **1995**, *100*, 18803.
(15) Vaida, V.; Kjaergaard, H. G.; Hintze, P. E.; Donaldson, D. J. *Science* **2003**, *299*, 1566.
(16) Sennikov, P. G.; Ignatov, S. K.; Schrems, O. *Chem. Phys. Chem.* **2005**, *6*, 392.
(17) Staikova, M.; Donaldson, D. J. *Phys. Chem. Earth (C)* **2001**, *26*, 473.
(18) Aloisio, S.; Francisco, J. S. *Acc. Chem. Res*. **2000**, *33*, 825.
(19) Pickering, S. U. *J. Chem. Soc.* **1893**, *63*, 436.
(20) (a) Luzzati, V. *Acta Crystallogr*. **1951**, *4*, 239. (b) Luzzati, V. *Acta Crystallogr*. **1953**, *6*, 152. (c) Luzzati, V. *Acta Crystallogr*. **1953**, *6*, 157.
(21) Delaplane, R. G.; Taesler, I.; Olovsson, I. *Acta Crystallogr*. **1975**, *B31*, 1486.
(22) Taesler, I.; Delaplane, R. G.; Olovsson, I. *Acta Crystallogr*. **1975**, *B31*, 1489.
(23) Ritzhaupt, G.; Devlin, J. P. *J. Phys. Chem*. **1991**, *95*, 90.
(24) (a) Tolbert, M. A.; Middlebrook, A. M. *J. Geophys. Res. D* **1990**, *95*, 22423. (b) Tolbert, M. A.; Koehler, B. G.; Middlebrook, A. M. *Spectrochim. Acta A* **1992**, *48A*, 1303.
(25) (a) Lebrun, N.; Mahe, F.; Lamiot, J.; Foulon, M.; Petit, J. C.; Prevost, D. *Acta Crystallogr. B* **2001**, *57*, 27. (b) Lebrun, N.; Mahe, F.; Lamiot, J.; Foulon, M.; Petit, J. C. *Acta Crystallogr. C* **2001**, *57*, 1129.
(26) Tizek, H.; Knözinger, E.; Grothe, H. *Phys. Chem. Chem. Phys*. **2002**, *4*, 5128.
(27) Beyer, K. D.; Hansen, A. R. *J. Phys. Chem. A* **2002**, *106*, 10275.
(28) Ji, K.; Petit, J. C.; Négrier, P.; Haget, Y. *Geophys. Res. Lett*. **1996**, *23*, 981.
(29) Barton, N.; Rowland, B.; Devlin, J. P. *J. Phys. Chem*. **1993**, *97*, 5848.
(30) (a) Ott, M. E.; Leopold, K. R. *J. Phys. Chem. A* **1999**, *103*, 1322. (b) Ott, M. E. Ph.D. Thesis, University of Minnesota, Minneapolis, MN, 1999.
(31) Li, Q.; Huber, J. R. *Chem. Phys. Lett*. **2001**, *345*, 415.
(32) Tsias, A.; Prenni, A. J.; Carslaw, K. S.; Onasch, T. P.; Luo, B. P.; Tolbert, M. A.; Peter, Th. *Geophys. Res. Lett*. **1997**, *24*, 2303.
(33) Richwine, L. J.; Clapp, M. L.; Miller, R. E.; Worsnop, D. R. *Geophys. Res. Lett*. **1995**, *22*, 2625.
(34) Curtius, J.; Froyd, K. D.; Lovejoy, E. R. *J. Phys. Chem. A* **2001**, *105*, 10867.
(35) Zhang, X.; Mereand, E. L.; Castleman, A. W., Jr. *J. Phys. Chem*. **1994**, *98*, 3554.
(36) Kobara, H.; Wakisaka, A.; Takeuchi, K.; Ibusuki, T. *J. Phys. Chem. A* **2002**, *106*, 4779.
(37) Tizek, H.; Knözinger, E.; Grothe, H. *Phys. Chem. Chem. Phys.* **2004**, *6*, 972.
(38) Grothe, H.; Myhre, C. E. L.; Tizek, H. *Vibr. Spectrosc*. **2004**, *34*, 55.
(39) Dickens, D. B.; Sloan, J. J. *J. Phys. Chem. A* **2002**, *106*, 10543; **2002**, *106*, 9736.
(40) Niedziela, R. F.; Miller, R. E.; Worsnop, D. R. *J. Phys. Chem. A* **1998**, *102*, 6477.
(41) Smith, R. H.; Leu, M.-T.; Keyser, L. F. *J. Phys. Chem*. **1991**, *95*, 5924.
(42) Koehler, B. G.; Middlebrook, A. M; Tolbert, M. A. *J. Geophys. Res. D* **1992**, *97*, 8065.
(43) Molina, M. J.; Zhang, R.; Wooldridge, P. J.; McMahon, J. R.; Kim, J. E.; Chang, H. Y.; Beyer, K. D. *Science* **1993**, *261*, 1418.
(44) Marti, J. J.; Mauersberger, K. *J. Phys. Chem*. **1994**, *98*, 6897.
(45) Ritzhaupt, G.; Devlin, J. P. *J. Phys. Chem*. **1977**, *81*, 521.
(46) Barnes, A. J.; Lasson, E.; Nielsen, C. J. *J. Mol. Struct*. **1994**, *322*, 165.
(47) Krajewska, M.; Mielke, Z. *Polish J. Chem*. **1998**, *72*, 335.
(48) (a) Bogdan, A.; Kulmala, M.; MacKenzie, A. R.; Laaksonen, A. *J. Geophys. Res*. **2003**, *108D*, 4303. (b) Bogdan, A.; Molina, M. J.; Kulmala, M.; MacKenzie, A. R.; Laaksonen, A. *J. Geophys. Res*. **2003**, *108D*, 4302.
(49) Latajka, Z.; Szczeœniak, M. M.; Ratajczak, H.; Orville-Thomas, W. J. *J. Comput. Chem*. **1980**, *1*, 417.
(50) Koller, J.; Hadži, D. *J. Mol. Struct*. **1991**, *247*, 225.
(51) Aloisio, S.; Francisco, J. S. *J. Phys. Chem. A* **1999**, *103*, 6049.
(52) Beichert, P.; Schrems, O. *J. Phys. Chem. A* **1998**, *102*, 10540.
(53) Kjaergaard, H. G. *J. Phys. Chem. A* **2002**, *106*, 2979.
(54) Sullivan, D. M.; Bagchi, K.; Tuckerman, M. E.; Klein, M. L. *J. Phys. Chem. A* **1999**, *103*, 8678.
(55) Fernández, D.; Botella, V.; Herrero, V. J.; Escribano, R**.** *J. Phys. Chem. B* **2003**, *107*, 10608.
(56) Staikova, M.; Donaldson, D. J. *Phys. Chem. Chem. Phys*. **2001**, *3*, 1999.
(57) Dimitrova, Y.; Peyerimhoff, S. *Chem. Phys*. **2000**, *254*, 125.
(58) Poshusta, R. D.; Tseng, D. C.; Hess, A. C.; McCarthy, M. I. *J. Phys. Chem.* **1993**, *97*, 7295.
(59) (a) Phillips, J. A.; Canagaratna, M.; Goodfriend, H.; Grushow, A.; Almlöf, J.; Leopold, K. R. *J. Am. Chem. Soc*. **1995**, *117*, 12549. (b) Phillips, J. A. Ph.D. Thesis, University of Minnesota, Minneapolis, MN 1996.
(60) Phillips, J. A.; Canagaratna, M.; Goodfriend, H.; Leopold, K. R. *J. Phys. Chem*. **1995**, *99*, 501.
(61) Hunt, S. W.; Higgins, K. J.; Craddock, M. B.; Brauer, C. S.; Leopold, K. R. *J. Am. Chem. Soc.* **2003**, *125*, 13850.
(62) Chilton, T. H. *Strong Water Nitric Acid: Sources, Method of Manufacture, and Uses;* MIT Press: Cambridge, MA, 1968; p 166.
(63) Craddock, M. B. Ph.D. Thesis, University of Minnesota, Minneapolis, MN, 2005.
(64) Gordy, W.; Cook, R. L. *Microwave Molecular Spectra*; John Wiley and Sons: New York, 1984.
(65) As a check, five a-type rotational transitions of the "A-state" of $HNO_3\cdots H_2O$ we re-fit and found to predict the b-type spectra of that species to within 2 MHz. Additionally, checks of this nature were run by fitting just a few a-type lines (for a given state) of $HCl\cdots(H_2O)_2$[66a] and subsequently predicting b-type rotational transitions and $^{35/37}$Cl hyperfine structure. In this case, too, b-type spectra were predicted to within a couple of MHz (or better) and $^{35/37}$Cl hyperfine was also predicted well compared with what was observed.
(66) (a) Kisiel, Z.; Bailkowska-Jaworska, E.; Pszczółkowski, L.; Milet, A.; Struniewicz, C.; Moszynski, R.; Sadlej, J. *J. Chem. Phys.* **2000**, *112*, 5767. (b) Kisiel, Z.; Pietrewicz, B. A.; Desyatnyk, O.; Pszczółkowski, L.; Strunicwicz, I.; Sadlej, J. *J. Chem. Phys.* **2003**, *119*, 5907.
(67) Xantheas, S. Private communication.
(68) Scheiner, S.; Ĉuma, M. *J. Am. Chem. Soc*. **1996**, *118*, 1511.

(69) Cox, A. P.; Riveros, J. M. *J. Chem. Phys.* **1965**, *42*, 3106.
(70) Cook, R. L.; De Lucia, F. C.; Helminger, P. *J. Mol. Spectrosc*. **1974**, *53*, 62.
(71) Kraitchman, J. *Am. J. Phys*. **1953**, *21*, 17.
(72) Kisiel, Z. *J. Mol. Spectrosc*. **2003**, *218*, 58.
(73) Albinus, L.; Spieckermann, J.; Sutter, D. H. *J. Mol. Spectrosc*. **1989**, *133*, 128.
(74) Ott., M. E.; Craddock, M. B.; Leopold, K. R. *J. Mol. Spectrosc.* **2005**, 229, 286.
(75) Dyke, T. R.; Mack, K. M.; Muenter, J. S. *J. Chem. Phys*. **1977**, *66*, 498.
(76) Kurnig, I. J.; Scheiner, S. *Int. J. Quantum Chem. Quantum Biol. Symp*. **1987**, *14*, 47.
(77) Brauer, C. S.; Craddock, M. B.; Kilian, J.; Grumstrup, E. M.; Orilall, M. C.; Mo, Y.; Gao, J.; Leopold, K. R. *J. Phys. Chem. A* **2006**, *110*, 10025.
(78) Sears, T. J.; Bunker, P. R.; Davies, P. B.; Johnson, S. A.; Širko, V. *J. Chem. Phys*. **1985**, *83*, 2676. Technically, we have used the experimental bond length for D_3O^+, but to the two decimal place accuracy to which we quote ρ_{PT}, this should not introduce significant error.
(79) Odutola, J. A.; Dyke, T. R. *J. Chem. Phys*. **1980**, *72*, 5062.
(80) Fiacco, D. L.; Hunt, S. W.; Leopold, K. R., *J. Am. Chem. Soc*. **2002**, 124, 4504.
(81) Kisiel, Z.; Pietrewicz, B. A.; Fowler, P. W.; Legon, A. C; Steiner, E. *J. Phys. Chem. A* **2000**, *104*, 6970.
(82) Legon, A. C.; Suckley, A. P. *Chem. Phys. Lett.* **1988**, *150*, 153.
(83) In doing these calculations, ab initio values of $(r_{HX} - r^o_{HX})$ have been estimated from previously published work: (a) Conley, C.; Tao, F.-M. *Chem. Phys. Lett*. **1999**, *301*, 29. (b) Re, S.; Osamura, Y.; Suzuk, Y.; Schaefer, H. F., III. *J. Chem. Phys*. **1998**, *109*, 973.
(84) Proton affinities are obtained from the National Institute of Standards and Technology online database: http://webbook.nist.gov/chemistry/.